

Binuclear Mesogenic Copper(I) Isocyanide Complexes with an Unusual Inorganic Core Formed by Two Tetrahedra Sharing an Edge

Mohamed Benouazzane, Silverio Coco, and Pablo Espinet*

Departamento de Química Inorgánica, Facultad de Ciencias, Universidad de Valladolid, E-47005 Valladolid, Spain

Joaquín Barberá

Departamento de Química Orgánica, Facultad de Ciencias-ICMA, Universidad de Zaragoza-CSIC, E-50009 Zaragoza, Spain

Received May 8, 2002

The preparation of binuclear mesogenic copper(I) isocyanide complexes $[\text{CuX}(\text{CNR})_2]_2$ ($\text{X} = \text{halogen}$; $\text{R} = \text{C}_6\text{H}_4\text{C}_6\text{H}_4\text{-OC}_{10}\text{H}_{21}$ (L^{A}), $\text{C}_6\text{H}_4\text{COOC}_6\text{H}_4\text{OC}_n\text{H}_{2n+1}$ (L^{B}), $\text{C}_6\text{H}_2(3,4,5\text{-OC}_n\text{H}_{2n+1})_3$ (L^{C})) with an unusual tetrahedral core is described. The copper complexes with L^{A} are not liquid crystals, but the Cu-L^{B} complexes show SmA mesophases and the Cu-L^{C} derivatives display hexagonal columnar mesophases, some of them at room temperature. The relationship between the molecular structure of the complexes and their thermal behavior is discussed.

Introduction

Many liquid crystals with metal-containing molecules (metallomesogens) have been synthesized, and molecular design and synthesis of mesogenic metal complexes with new structures or improved physical properties constitute an active research area.^{1–10} The most popular molecular design to build liquid crystals is that confining the core and the chains of the molecule near a plane. So aromatic rings linked by conjugated spacers that give rise to rodlike molecules (Figure 1a) are very common structures in organic liquid crystals. The same idea is often applied to metallomesogens, although these can produce liquid crystals with less appropriate molecular shapes. Complexes based on square

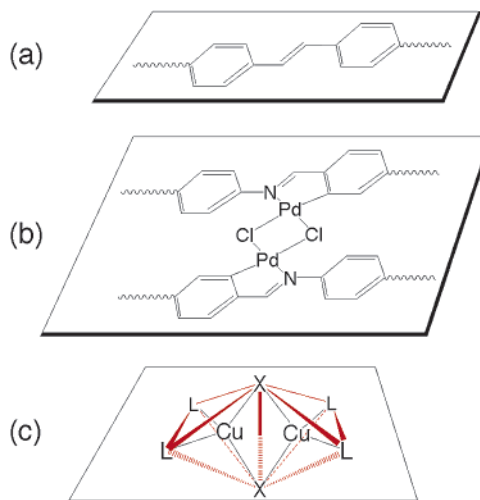


Figure 1. Typical liquid crystal molecular shapes: (a) organic rodlike molecules; (b) metallomesogens based on square planar coordination around the metal. The shape of the molecules prepared in this paper (c) can be considered atypical.

planar coordination around the metal are particularly suited. The dimer shown in Figure 1b represents a particularly successful structural type that has given rise to hundreds of metallomesogens,^{4,7} but the plethora of ligands and metals that can be used in this field has provided a rich structural diversity of metal complexes showing liquid crystal behavior. These include apparently unfavorable geometries such as

* To whom correspondence should be addressed. E-mail: espinet@qi.uva.es.

- (1) Espinet, P.; Esteruelas, M. A.; Oro, L. A.; Serrano, J. L.; Sola, E. *Coord. Chem. Rev.* **1992**, *117*, 215.
- (2) Bruce, D. W. In *Inorganic Materials*, 2nd ed.; Bruce D. W., D. O'Hare, D., Eds.; Wiley: Chichester, U.K., 1996; Chapter 8.
- (3) Hudson, S. A.; Maitlis, P. M. *Chem. Rev.* **1993**, *93*, 861.
- (4) *Metallomesogens*; Serrano, J. L., Ed.; VCH: Weinheim, Germany, 1996.
- (5) Oriol, L.; Serrano, J. L. *Adv. Mater.* **1995**, *7*, 348.
- (6) Giroud-Godquin, A. M. *Coord. Chem. Rev.* **1998**, *180*, 1481.
- (7) Donnio, B.; Bruce, D. W. *Struct. Bonding* **1999**, *95* (Liquid Crystals II), 193.
- (8) Espinet, P. *Gold Bull.* **1999**, *32*, 127.
- (9) Collison, S.; Bruce, D. W. In *Transition Metals in Supramolecular Chemistry*; Sauvage, J. P., Ed.; Wiley: Chichester, U.K., 1999; Chapter 7.
- (10) Bruce, D. W. *Adv. Inorg. Chem.* **2001**, *52*, 151.

tetrahedral nickel(II)^{11–13} and Cu(I) complexes,¹⁴ some octahedral derivatives of several transition metals,^{15–20} distorted square-pyramidal complexes of iron^{21–23} and vanadyl,²⁴ a few Co, Cu, Zn, and Fe trigonal-bipyramidal complexes,^{25,26} and zirconium square-antiprismatic compounds.²⁷

A novel promising structural metalcore for metallomesogens might be that represented in Figure 1c, since it sets the four coordination positions for the promesogenic ligands in a plane. A structure of this type has been determined by X-ray diffraction for binuclear copper isocyanide complexes [CuX(CNR)₂]₂ (X = halogen; R = alkyl or aryl group).²⁸ We decided to explore this structural motif because it appears in the chemistry of a number of transition metals and might open a rather wide field for future work. Moreover, isocyanide is a particularly appropriate ligand to prepare liquid crystals, since it gives very stable complexes with many transition metals in different oxidation states. The diversity of liquid crystal based on isocyanide metal complexes includes linear copper(I),²⁹ silver(I),³⁰ and gold(I)^{31–39} compounds, cis and trans square-planar palladium(II) and plati-

num(II) derivatives,^{40–43} and trigonal bipyramidal iron(0) complexes.²⁶ In this paper we describe the preparation and liquid crystal behavior of binuclear copper(I) isocyanide complexes [CuX(CNR)₂]₂ (X = halogen; R = C₆H₄C₆H₄OC₁₀H₂₁ (L^A), C₆H₄COOC₆H₄OC_nH_{2n+1} (L^B), C₆H₂(3,4,5-OC_nH_{2n+1})₃ (L^C)).

Experimental Section

Materials and Reagents. Literature methods were used to prepare CNR (R = C₆H₄C₆H₄OC_nH_{2n+1},³³ C₆H₄COOC₆H₄OC_nH_{2n+1},⁴¹ C₆H₄OOCC₆H₄OC_nH_{2n+1},⁴¹ C₆H₂(3,4,5-OC_nH_{2n+1})₃; n = 4, 6, 8, 10, 12)³⁷ and CuCl.⁴⁴ Instrumentation was as described elsewhere.²⁶

XRD measurements were performed with a pinhole camera (Anton-Paar) operating with a point-focused Ni-filtered Cu K α beam. The sample was held in Lindemann glass capillaries (1 mm diameter) and heated, when necessary, with a variable-temperature attachment. The patterns were collected on flat photographic film. The capillary axis and the film are perpendicular to the X-ray beam. Spacings are obtained via Bragg's law.

Only examples procedures are described, as the syntheses were similar for the rest of the compounds. Yields, IR, and analytical data are given for all the copper complexes.

Preparation of [CuX(CNR)₂]₂ [X = Cl, Br, I; R = C₆H₄C₆H₄OC_nH_{2n+1}, C₆H₄COOC₆H₄OC_nH_{2n+1}, C₆H₂(3,4,5-OC_nH_{2n+1})₃]. To a dichloromethane (40 mL) suspension of CuX (X = Cl, Br, I) (0.5 mmol), under an atmosphere of nitrogen, was added 2 equiv of the corresponding isocyanide (1.1 mmol). After being stirred for 1 h, the resulting solution was filtered in air and hexane (10 mL) was added. The solution was concentrated, which afforded the corresponding compounds as white solids, except the chloro and bromo derivatives that appear as yellow solids.

Yields, IR, analytical data, and representative ¹H NMR follow below. When ¹H NMR are not given, these are practically identical to those provided for similar complexes (except for the intensity of the multiplet comprising the undefined hydrogens of the alkoxy chains, which is in each case proportional to their number).

R = C₆H₄C₆H₄OC₁₀H₂₁ (Cu–L^A). X = Cl. Yield: 92%. IR (Nujol) [$\nu(\text{C}\equiv\text{N})/\text{cm}^{-1}$]: 2136 s, 2161 s. ¹H NMR (CDCl₃): δ_1 7.63, δ_2 7.72, AA'XX' spin system ($^3J_{1,2} + ^5J_{1,2} = 8.6$ Hz), δ_3 7.63, δ_4 7.12, AA'XX' spin system ($^3J_{3,4} + ^5J_{3,4} = 8.7$ Hz), 4.14 (t, J = 6.5 Hz, OCH), 2.00–1.01 (m, 19H, alkoxy chain). Anal. Calcd for C₉₂H₁₁₆Cl₂Cu₂N₄O₄: C, 71.76; H, 7.59; N, 3.64. Found: C, 71.47; H, 7.53; N, 3.84.

X = Br. Yield: 61%. IR (Nujol) [$\nu(\text{C}\equiv\text{N})/\text{cm}^{-1}$]: 2153 s. Anal. Calcd for C₉₂H₁₁₆Br₂Cu₂N₄O₄: C, 67.84; H, 7.18; N, 3.44. Found: C, 67.91; H, 7.23; N, 3.54.

X = I. Yield: 71%. IR (Nujol) [$\nu(\text{C}\equiv\text{N})/\text{cm}^{-1}$]: 2151 s. Anal. Calcd for C₉₂H₁₁₆Cu₂I₂N₄O₄: C, 64.14; H, 6.79; N, 3.25. Found: C, 64.09; H, 6.74; N, 3.54.

R = C₆H₄COOC₆H₄OC_nH_{2n+1} (Cu–L^B). X = Cl. n = 4. Yield: 69%. IR (Nujol) [$\nu(\text{C}\equiv\text{N})/\text{cm}^{-1}$]: 2146 s, 2165 s. ¹H NMR (CDCl₃): δ_1 7.60, δ_2 8.25, AA'XX' spin system ($^3J_{1,2} + ^5J_{1,2} = 8.5$ Hz), δ_3 7.09, δ_4 6.92, AA'XX' spin system ($^3J_{3,4} + ^5J_{3,4} = 9.0$ Hz), 3.96 (t, J = 6.5 Hz, OCH₂), 1.79–0.95 (m, 7H, alkoxy chain). Anal. Calcd for C₇₂H₆₄Cl₂Cu₂N₄O₁₂: C, 62.70; H, 4.97; N, 4.06. Found: C, 62.57; H, 5.05; N, 4.01.

- (11) Griesar, K.; Galyametdinov, Y.; Athanassopoulou, M.; Ouchinnikov, I.; Haase, W. *Adv. Mater.* **1994**, *6*, 381.
- (12) Pyzuk, W.; Galyametdinov, Y. *Liq. Cryst.* **1993**, *15*, 265.
- (13) Mehl, G. H.; Goodby, J. W. *Chem. Ber.* **1996**, *129*, 521.
- (14) (a) El-Ghayoury, A.; Douce, L.; Skoulios, A.; Ziessel, R. *Angew. Chem., Int. Ed.* **1998**, *37*, 2205. (b) Neve, F.; Ghedini, M.; Levelut, A. M.; Francescangeli, O. *Chem. Mater.* **1994**, *6*, 70.
- (15) Lattermann, G.; Schmidt, S.; Kleppinger, R.; Wendorff, J. H. *Adv. Mater.* **1992**, *4*, 30.
- (16) Bruce, D. W.; Lin, X. H. *J. Chem. Soc., Chem. Commun.* **1994**, 729.
- (17) Zheng, H.; Swager, T. M. *J. Am. Chem. Soc.* **1994**, *116*, 761.
- (18) Rove, K. E.; Bruce, D. W. *J. Chem. Soc., Dalton Trans.* **1996**, 3913.
- (19) Giroud-Godquin, A. M.; Rassat, A.; Séances, C. R. *Acad. Sci. Ser.* **1982**, *2*, 241.
- (20) Deschenaux, R.; Marandaz, J. L. *J. Chem. Soc., Chem. Commun.* **1991**, 909.
- (21) Haase, W.; Griesar, K.; Iskander, M. F.; Galyametdinov, Y. *Mol. Cryst. Liq. Cryst., Sect. C* **1993**, *171*, 1.
- (22) Galyametdinov, Y.; Ivanovo, G.; Griesar, K.; Prosvirin, A.; Ouchinnikov, I.; Haase, W. *Adv. Mater.* **1992**, *3*, 115.
- (23) Marcos, M.; Serrano, J. L.; Alonso, P. J.; Martínez, J. I. *Adv. Mater.* **1995**, *173*.
- (24) Campillos, E.; Marcos, M.; Omenat, A.; Serrano, J. L. *J. Mater. Chem.* **1996**, *6*, 349.
- (25) Stebani, U.; Lattermann, G.; Wittenberg, M.; Wendorff, J. H. *Angew. Chem., Int. Ed. Engl.* **1996**, *35*, 1858.
- (26) Coco, S.; Espinet, P.; Marcos, E. *J. Mater. Chem.* **2000**, *10*, 1297.
- (27) Trzaska, S. T.; Zheng, H.; Swager, T. M. *Chem. Mater.* **1999**, *11*, 130.
- (28) Toht, A.; Floriani, C. *J. Chem. Soc., Dalton Trans.* **1988**, 1599.
- (29) Benouazzane, M.; Coco, S.; Espinet, P.; Barberá, J. *J. Mater. Chem.* **2001**, *11*, 1740.
- (30) Benouazzane, M.; Coco, S.; Espinet, P.; Barberá, J. *J. Mater. Chem.* **2002**, *12*, 691.
- (31) Kaharu, T.; Ishii, R.; Takahashi, S. *J. Chem. Soc., Chem. Commun.* **1994**, 1349.
- (32) Kaharu, T.; Ishii, R.; Adachi, T.; Yoshida, T.; Takahashi, S. *J. Mater. Chem.* **1995**, *5*, 687.
- (33) Benouazzane, M.; Coco, S.; Espinet, P.; Martín-Álvarez, J. M. *J. Mater. Chem.* **1995**, *5*, 441.
- (34) Coco, S.; Espinet, P.; Falagán, S.; Martín-Álvarez, J. M. *New J. Chem.* **1995**, *19*, 959.
- (35) Alejos, P.; Coco, S.; Espinet, P. *New J. Chem.* **1995**, *19*, 799.
- (36) Bayón, R.; Coco, S.; Espinet, P.; Fernández-Mayordomo, C.; Martín-Álvarez, J. M. *Inorg. Chem.* **1997**, *36*, 2329.
- (37) Coco, S.; Espinet, P.; Martín-Álvarez, J. M.; Levelut, A. M. *J. Mater. Chem.* **1997**, *7*, 19.
- (38) Benouazzane, M.; Coco, S.; Espinet, P.; Martín-Álvarez, J. M. *J. Mater. Chem.* **1999**, *9*, 2327.
- (39) Omenat, A.; Serrano, J. L.; Sierra, T.; Amabilino, D. B.; Minquet, M.; Ramos, E.; Veciana, J. *J. Mater. Chem.* **1999**, *9*, 2301.

- (40) Kaharu, T.; Takahashi, S. *Chem. Lett.* **1992**, 1515.
- (41) Kaharu, T.; Tanaka, T.; Sawada, M.; Takahashi, S. *J. Mater. Chem.* **1994**, *4*, 859.
- (42) Coco, S.; Díez-Expósito, F.; Espinet, P.; Fernández-Mayordomo, C.; Martín-Álvarez, J. M.; Levelut, A. M. *Chem. Mater.* **1998**, *10*, 3666.
- (43) Wang, S.; Mayr, A.; Cheung, K. K. *J. Mater. Chem.* **1998**, *8*, 1561.
- (44) Kauffman, G. B.; Pinnell, R. P. *Inorg. Synth.* **1960**, *6*, 3.

$n = 6$. Yield: 58%. IR (Nujol) [$\nu(\text{C}\equiv\text{N})/\text{cm}^{-1}$]: 2146 s, 2165 s. Anal. Calcd for $\text{C}_{80}\text{H}_{80}\text{Cl}_2\text{Cu}_2\text{N}_4\text{O}_{12}$: C, 64.42; H, 5.68; N, 3.76. Found: C, 64.69; H, 5.87; N, 3.65.

$n = 8$. Yield: 64%. IR (Nujol) [$\nu(\text{C}\equiv\text{N})/\text{cm}^{-1}$]: 2146 s, 2165 s. Anal. Calcd for $\text{C}_{88}\text{H}_{96}\text{Cl}_2\text{Cu}_2\text{N}_4\text{O}_{12}$: C, 65.91; H, 6.29; N, 3.49. Found: C, 65.91; H, 6.35; N, 3.36.

$n = 10$. Yield: 60%. IR (Nujol) [$\nu(\text{C}\equiv\text{N})/\text{cm}^{-1}$]: 2147 s, 2166 s. Anal. Calcd for $\text{C}_{96}\text{H}_{112}\text{Cl}_2\text{Cu}_2\text{N}_4\text{O}_{12}$: C, 67.20; H, 6.81; N, 3.27. Found: C, 67.50; H, 7.05; N, 3.16.

$n = 12$. Yield: 85%. IR (Nujol) [$\nu(\text{C}\equiv\text{N})/\text{cm}^{-1}$]: 2147 s, 2165 s. Anal. Calcd for $\text{C}_{104}\text{H}_{128}\text{Cl}_2\text{Cu}_2\text{N}_4\text{O}_{12}$: C, 68.33; H, 7.28; N, 3.07. Found: C, 68.69; H, 7.62; N, 2.97.

$\text{X} = \text{Br}$. $n = 4$. Yield: 62%. IR (Nujol) [$\nu(\text{C}\equiv\text{N})/\text{cm}^{-1}$]: 2145 s, 2158 s. Anal. Calcd for $\text{C}_{72}\text{H}_{64}\text{Br}_2\text{Cu}_2\text{N}_4\text{O}_{12}$: C, 58.90; H, 4.67; N, 3.82. Found: C, 59.14; H, 4.88; N, 3.82.

$n = 12$. Yield: 50%. IR (Nujol) [$\nu(\text{C}\equiv\text{N})/\text{cm}^{-1}$]: 2142 s, 2158 s. Anal. Calcd for $\text{C}_{104}\text{H}_{128}\text{Br}_2\text{Cu}_2\text{N}_4\text{O}_{12}$: C, 65.16; H, 6.94; N, 2.92. Found: C, 65.11; H, 6.89; N, 3.08.

$\text{X} = \text{I}$. $n = 4$. Yield: 61%. IR (Nujol) [$\nu(\text{C}\equiv\text{N})/\text{cm}^{-1}$]: 2136 s, 2158 s. Anal. Calcd for $\text{C}_{72}\text{H}_{64}\text{Cu}_2\text{I}_2\text{N}_4\text{O}_{12}$: C, 55.37; H, 4.39; N, 3.59. Found: C, 55.48; H, 4.42; N, 3.46.

$n = 12$. Yield: 50%. IR (Nujol) [$\nu(\text{C}\equiv\text{N})/\text{cm}^{-1}$]: 2136 s, 2159 s. Anal. Calcd for $\text{C}_{104}\text{H}_{128}\text{Cu}_2\text{I}_2\text{N}_4\text{O}_{12}$: C, 62.11; H, 6.62; N, 2.79. Found: C, 62.26; H, 6.59; N, 3.00.

$\text{R} = \text{C}_6\text{H}_2(3,4,5\text{-OC}_n\text{H}_{2n+1})_3$ (Cu-L^{C}). $\text{X} = \text{Cl}$. $n = 4$. Yield: 83%. IR (Nujol) [$\nu(\text{C}\equiv\text{N})/\text{cm}^{-1}$]: 2158 s. ^1H NMR (CDCl_3): δ 6.64 (s, $J = 2\text{H}$, C_6H_2), 3.93 (m, 6H, OCH_2), 1.83–0.92 (m, 21H, *alkoxy chains*). Anal. Calcd for $\text{C}_{76}\text{H}_{116}\text{Cl}_2\text{Cu}_2\text{N}_4\text{O}_{12}$: C, 61.86; H, 7.92; N, 3.80. Found: C, 61.56; H, 7.71; N, 3.79.

$n = 6$. Yield: 58%. IR (Nujol) [$\nu(\text{C}\equiv\text{N})/\text{cm}^{-1}$]: 2170 s. Anal. Calcd for $\text{C}_{100}\text{H}_{164}\text{Cl}_2\text{Cu}_2\text{N}_4\text{O}_{12}$: C, 66.27; H, 9.12; N, 3.09. Found: C, 66.55; H, 8.87; N, 3.29.

$n = 8$. Yield: 65%. IR (Nujol) [$\nu(\text{C}\equiv\text{N})/\text{cm}^{-1}$]: 2158 s. Anal. Calcd for $\text{C}_{124}\text{H}_{212}\text{Cl}_2\text{Cu}_2\text{N}_4\text{O}_{12}$: C, 69.30; H, 9.94; N, 2.61. Found: C, 69.12; H, 9.77; N, 2.99.

$n = 10$. Yield: 58%. IR (Nujol) [$\nu(\text{C}\equiv\text{N})/\text{cm}^{-1}$]: 2171 s. Anal. Calcd for $\text{C}_{148}\text{H}_{260}\text{Cl}_2\text{Cu}_2\text{N}_4\text{O}_{12}$: C, 71.51; H, 10.54; N, 2.25. Found: C, 71.58; H, 10.32; N, 2.57.

$n = 12$. Yield: 63%. IR (Nujol) [$\nu(\text{C}\equiv\text{N})/\text{cm}^{-1}$]: 2168 s. Anal. Calcd for $\text{C}_{172}\text{H}_{308}\text{Cl}_2\text{Cu}_2\text{N}_4\text{O}_{12}$: C, 73.20; H, 11.00; N, 1.99. Found: C, 72.91; H, 10.89; N, 2.01.

$\text{X} = \text{Br}$. $n = 4$. Yield: 87%. IR (Nujol) [$\nu(\text{C}\equiv\text{N})/\text{cm}^{-1}$]: 2152 s. Anal. Calcd for $\text{C}_{76}\text{H}_{116}\text{Br}_2\text{Cu}_2\text{N}_4\text{O}_{12}$: C, 58.34; H, 7.47; N, 3.58. Found: C, 58.43; H, 7.32; N, 3.53.

$n = 12$. Yield: 75%. IR (Nujol) [$\nu(\text{C}\equiv\text{N})/\text{cm}^{-1}$]: 2159 s. Anal. Calcd for $\text{C}_{172}\text{H}_{308}\text{Br}_2\text{Cu}_2\text{N}_4\text{O}_{12}$: C, 70.96; H, 10.66; N, 1.92. Found: C, 70.72; H, 10.37; N, 1.93.

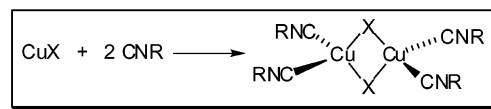
$\text{X} = \text{I}$. $n = 4$. Yield: 83%. IR (Nujol) [$\nu(\text{C}\equiv\text{N})/\text{cm}^{-1}$]: 2154 s. Anal. Calcd for $\text{C}_{76}\text{H}_{116}\text{Cu}_2\text{I}_2\text{N}_4\text{O}_{12}$: C, 55.03; H, 7.05; N, 3.38. Found: C, 55.32; H, 6.82; N, 3.57.

$n = 12$. Yield: 76%. IR (Nujol) [$\nu(\text{C}\equiv\text{N})/\text{cm}^{-1}$]: 2161 s. Anal. Calcd for $\text{C}_{172}\text{H}_{308}\text{Cu}_2\text{I}_2\text{N}_4\text{O}_{12}$: C, 68.74; H, 10.33; N, 1.86. Found: C, 68.97; H, 10.03; N, 1.66.

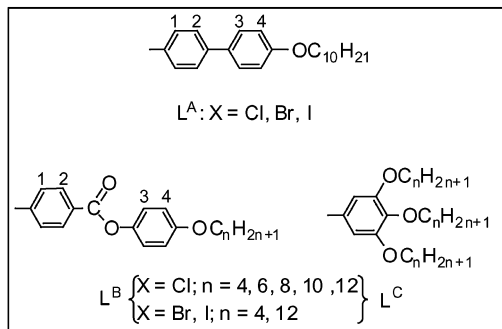
Results and Discussion

Synthesis and Structural Characterization. Binuclear complexes $[\text{CuX}(\text{CNR})_2]_2$ ($\text{X} = \text{halogen}$; $\text{R} = \text{C}_6\text{H}_4\text{C}_6\text{H}_4\text{-OC}_{10}\text{H}_{21}$ (L^{A}), $\text{C}_6\text{H}_4\text{COOC}_6\text{H}_4\text{OC}_n\text{H}_{2n+1}$ (L^{B}), $\text{C}_6\text{H}_2(3,4,5\text{-OC}_n\text{H}_{2n+1})_3$ (L^{C})) were prepared according to Scheme 1. C, H, and N analyses for the complexes, yields, and relevant IR data are given in the Experimental Section.

Scheme 1



$\text{R} =$



Their IR spectra show two $\nu(\text{C}\equiv\text{N})$ absorptions (D_{2h} , B_{2u} + B_{3u}) for the isocyanide groups, at higher wavenumbers (ca. 60 cm^{-1}) than for the free isocyanide, as reported for similar *p*-tolyl isocyanide complexes.²⁸ Some show only one $\nu(\text{C}\equiv\text{N})$ absorption, possibly due to overlapping of two expected bands.

The ^1H NMR spectra of the metal complexes are all very similar for each family. L^{A} and L^{B} derivatives, show, as expected, four somewhat distorted “pseudodoublets” (a deceptively simple pattern for the $\text{AA}'\text{XX}'$ spin systems) for the two phenyl groups present in the molecule. In addition, the first methylene group of the alkoxy chain is observed as a triplet at 3.9–4.1 ppm. The remaining chain hydrogens appear in the range 0.8–1.8 ppm. The ^1H NMR spectra of L^{C} complexes show one signal from aromatic protons, corresponding to the two equivalent protons present in the molecule.

Mesogenic Behavior. The free isocyanides L^{A} and L^{B} display nematic and/or smectic A phases in the range 60–90 °C.⁴⁰ However, only the Cu derivatives with L^{B} are mesogenic. The copper derivatives of L^{A} look unpromising; those prepared were not liquid crystals, and more systematic variation of the chain was not undertaken. On the contrary, although the free L^{C} isocyanides are not liquid crystals, all their copper isocyanide complexes are mesogenic.

The optical, thermal, and thermodynamic data of complexes are collected in Table 1. The Cu– L^{B} derivatives display smectic A (SmA) mesophases, identified in optical microscopy by their typical myelinic and homeotropic textures that reorganize to produce fan-shaped focal-conic areas at temperatures close to the clearing point. When the length of the chain increases, the melting points of the chloro Cu– L^{B} derivatives do not change significantly, but the clearing temperatures decrease narrowing the range of SmA mesophase. The substitution of Cl by Br or I produces little variation in the melting points, but the mesogenic ranges cannot be compared because the clearing temperatures are, in fact, decomposition temperatures.

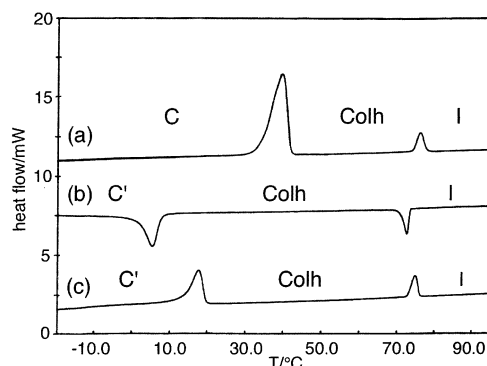
When 3,4,5-trialkoxyphenyl isocyanides are used, all the copper complexes prepared, Cu– L^{C} , display liquid crystal behavior, some of them at room temperature. The derivatives

Table 1. Optical, Thermal, and Thermodynamic Data for Complexes $[\text{Cu}_2(\mu\text{-X})_2(\text{CNR})_4]$

R	n	X	transition ^a	temp ^b (°C)	ΔH^b (kJ/mol)
L ^A	10	Cl	C → C'	105.5	2.8
			C' → I	167.2	96.1
L ^A	10	Br	C → I	164.7	75.1
L ^A	10	I	C → I	167.8	102.2
L ^B	4	Cl	C → C'	184.9	23.2
			C' → SmA	196.1	24.3
L ^B	6	Cl	SmA → I	267 (dec) ^c	
			C → SmA	187.4	57.2
L ^B	8	Cl	SmA → I	265 (dec) ^c	
			C → SmA	185.8	44.2
L ^B	10	Cl	SmA → I	270 (dec) ^c	
			C → SmA	179.4	45.7
L ^B	12	Cl	SmA → I	236 (dec) ^c	
			C → SmA	189.7	45.8
L ^B	4	Br	SmA → I	195 (dec) ^c	
			C → C'	138.3	-19.3
L ^B	12	Br	C' → SmA	191.4	73.6
			SmA → I	199 (dec) ^c	
L ^B	4	I	C → C'	99.2	26.7
			C' → C''	157.6	46.4
L ^B	12	I	C'' → SmA	185.9	58.7
			SmA → I	196 (dec) ^c	
L ^B	4	I	C → C'	109.9	7.1
			C' → SmA	188.5	74.4
L ^B	12	I	SmA → I	194 (dec) ^c	
			C → C'	146.6	3.6
L ^C	4	Cl	C' → C''	159.4	10.6
			C'' → SmA	177.5	52.8
L ^C	6	Cl	SmA → I	199 (dec) ^c	
			C → I	76.5 ^d	36.4
L ^C	8	Cl	I → Col _h	66.7	-5.2
			C → Col _h	29.2	5.5
L ^C	10	Cl	Col _h → I	83.9	7.6
			Col _i → Col _h	56.3	18.1
L ^C	12	Cl	Col _h → I	78.0	7.8
			Col _h → I	77.0	12.0
L ^C	4	Br	C → Col _h	13.9	48.8
			Col _h → I	72.9	14.1
L ^C	12	Br	C → I	78.9 ^d	24.3
			I → Col _h	70.2	-2.1
L ^C	4	I	C → C'	9.6	16.6
			C' → Col _h	27.0	8.5
L ^C	12	I	Col _h → I	75.2	5.8
			C → C'	74.7 ^d	4.3
L ^C	4	I	C' → I	88.1 ^d	17.9
			I → Col _h	51.9	1.4
L ^C	12	I	C → Col _h	13.7	45.9
			Col _h → I	82.2	10.9

^a Key: C, crystal; Sm, smectic; Col_h, hexagonal columnar; Col_i, rectangular columnar; I, isotropic liquid. ^b Data referred to the second DSC cycle starting from the crystal. Temperature data are at peak onset. ^c Microscopy data. ^d Data referred to the first DSC cycle.

with $n = 4$ are only monotropic. The optical textures, when viewed with a polarizing microscope on cooling from the isotropic melt, suggest columnar hexagonal phases and display linear birefringent defects, large areas of uniform extinction, and fan domains.⁴² In fact the high-temperature X-ray patterns of $[\text{CuCl}(\text{CNC}_6\text{H}_2(3,4,5\text{-OC}_8\text{H}_{17})_3)_2]_2$ and of the three compounds $[\text{CuX}(\text{CNC}_6\text{H}_2(3,4,5\text{-OC}_{12}\text{H}_{25})_3)_2]_2$ ($X = \text{Cl, Br, I}$) are consistent with a columnar hexagonal mesophase. The small-angle region contains a set of three or four reflections in a reciprocal spacing ratio $1:\sqrt{3}:\sqrt{4}:\sqrt{7}$. The hexagonal lattice constant deduced from the patterns is 27.7 \AA at $65 \text{ }^\circ\text{C}$ for $[\text{CuCl}(\text{CNC}_6\text{H}_2(3,4\text{-OC}_8\text{H}_{17})_3)_2]_2$ and $33.5 \pm 0.5 \text{ \AA}$ at $42 \text{ }^\circ\text{C}$ for the three compounds with dodecyloxy chains. From density estimations it is deduced that the columnar structure is generated by single molecules stacked at a mean distance of about 5 \AA . It is interesting to

**Figure 2.** DSC scans of $[\text{CuCl}(\text{CNC}_6\text{H}_2(3,4,5\text{-OC}_{12}\text{H}_{25})_3)_2]_2$: (a) first heating; (b) first cooling; (c) second heating.

note that the mesophase parameter increases with the chain length, as expected, but it does not vary, within the experimental error, upon changing the halogen atom. This suggests that the molecule thickness is determined essentially by the bulky trialkoxyphenyl groups. The three as-obtained compounds with dodecyloxy chains are crystalline, but upon cooling of the molten samples, the Col_h mesophase persists at room and below room temperature for $X = \text{Cl}$ and needs cooling to lower temperature to produce crystals. A second DSC heating scan produces the crystal–mesophase transition below room temperature and with a lower enthalpy exchange, as shown in Figure 2. This suggests that a different, metastable crystalline form (C) has been formed on cooling from the mesophase, different from the originally formed upon crystallization from the solution (C'). On the other hand, the chloro complex with octyloxy chains shows, in addition to a Col_h, a second mesophase at room temperature both in the original complex and in a previously molten sample. The X-ray patterns from this new phase can be indexed in a rectangular columnar structure with lattice constants $a = 48.5 \text{ \AA}$ and $b = 28 \text{ \AA}$ and two columns/unit cell. It is worth noting that the transition from the high-temperature mesophase to the low-temperature mesophase in this compound seems to produce only a slight distortion in the columnar arrangement, as a hexagonal lattice with $a = 27.7 \text{ \AA}$ is equivalent to a C-centered rectangular lattice with $a = 48 \text{ \AA}$, $b = 27.7 \text{ \AA}$ ($a/b = \sqrt{3}$), and two molecules/unit cell.

Discussion

The molecular structure of these compounds consists of two $[\text{CuCl}_2(\text{CNR})_2]$ tetrahedral copper centers sharing an edge that contains the two bridging halogens. This structure produces a planar arrangement of the other four coordination positions, which accommodate the four isocyanide groups. The two bridging halogens lay above and below this plane, as represented in Figure 3.²⁸

In the 3,4,5-trialkoxypheyl isocyanide derivatives, 12 alkyl chains are situated around the central core of the molecule, producing a disklike structure (Figure 4a) suitable to give rise to a columnar packing and display mesogenic behavior, as indeed observed. However, when the isocyanide used contains only one alkyl chain, calamitic mesophases are observed. This result can be understood considering that the arrangement beyond the double tetrahedral core can

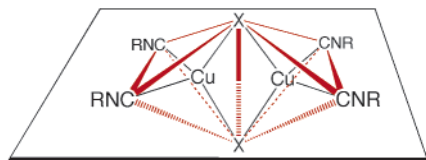


Figure 3. Structural core of the complexes $[\text{CuX}(\text{CNR})_2]_2$.

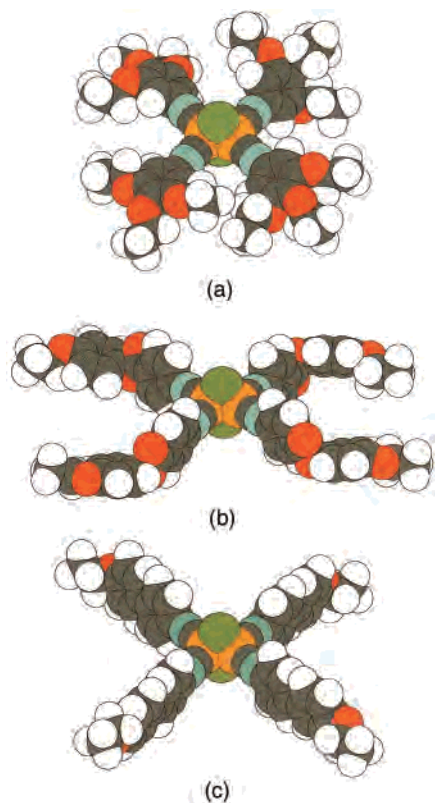


Figure 4. Space-filling model of the complexes $[\text{CuCl}(\text{CNR})_2]_2$ [(a) $\text{R} = \text{C}_6\text{H}_2(3,4,5\text{-OC}_2\text{H}_5)_3$; (b) $\text{C}_6\text{H}_4\text{COOC}_6\text{H}_4\text{OC}_2\text{H}_5$; (c) $\text{C}_6\text{H}_4\text{C}_6\text{H}_4\text{OC}_2\text{H}_5$], showing the structural variations introduced by the isocyanide.

become calamitic for isocyanide ligands that can adopt an adequate conformation. This is the case of the ligands L^{B} , which contain an ester moiety and can acquire a conformation where the second ring and its chain in the *para* position become aligned by pairs (Figure 4b). This conformation leads to the better space filling and intermolecular interactions. Thus, the molecular structure becomes calamitic, especially for long chain, and it is not unexpected that L^{B} copper derivatives show liquid crystal behavior.

On the contrary, for biphenyl isocyanide derivatives, the rigidity of biphenyl group does not permit one to obtain a conformation with a dominant cylindrical shape (Figure 4c). Only from the oxygen of the alkoxy chain, parallel conformation of the ligands suitable for mesogenic behavior becomes possible, but it is clear from Figure 3c that at this point the width of the molecule is too wide and the chains are too far away and would not fill the space efficiently, except if they curl. Consistently, the copper biphenyl isocyanide compounds are not liquid crystals.

Finally, it is interesting to analyze the effect of the halogen atoms. The substitution of Cl by Br and I in the L^{B} calamitic-

like copper derivatives, which show calamitic mesophases, produces a decrease in the transition temperatures in the order $\text{Cl} > \text{Br} > \text{I}$ for $n = 4$ and $\text{Br} > \text{Cl} > \text{I}$ for $n = 12$. In the L^{C} discotic-like complexes, which display columnar mesophases, the variation is the contrary, $\text{I} > \text{Br} > \text{Cl}$. To suggest a rationale for the observed thermal behavior, one can look at these molecules as initially planar, with two halogeno substituents located in the core of the molecule protruding out of the plane and the aryl and chain atoms filling the space close to that plane in such a way that an efficient molecular packing is achieved. Each $\text{X}-\text{M}$ -isocyanide moiety provides a complex multipolar leg of these four-legged molecules, with electrostatic results very difficult to predict. However, the experimental results can be understood assuming that the balance of charge interactions between $\text{X}-\text{M}$ -isocyanide moieties decreases in the order $\text{I} > \text{Br} > \text{Cl}$. Thus, the substitution of the chloro atoms by bromo or iodo would cause mainly two opposite effects: (i) a perturbation of the molecular distribution, which might increase the breadth of the molecule in the direction the halogens are protruding, affording lower transition temperatures for the heavier halogen; (ii) a decrease of the balance of charge interactions between $\text{X}-\text{M}$ -isocyanide, leading to higher transition temperatures for the heavier the halogen. The variation of transition temperatures versus halogen will be determined by the predominant factor.

Experimental evidence in calamitic organic liquid crystals (considered as a cylinders) shows that a decrease of intermolecular forces always predominates when the lateral substituent is bulky enough to increase and determine the breadth of the molecule.⁴⁵ Considering the X-ray structure determined for $[\text{CuCl}(\text{CNC}_6\text{H}_4\text{CH}_3\text{-}p)_2]_2$,²⁸ it is easy to conclude that in our monoalkylphenyl isocyanide copper derivatives (L^{B}) the breadth of the molecule should be determined by the size of the halogen. Consequently, lower transition temperatures should be obtained for the larger halo ligands, as observed. However, when the length of the alkoxy chain is increased, one might expect that the melt of the chains, not perfectly stretched since they have to fill the space between the parallel directions determined by the aryl rings, will increase the breadth of the molecule so as to make the size of the halogen unimportant for Cl and Br but still determinant for $\text{X} = \text{I}$. This may explain why the trend observed for $n = 12$ is $\text{Br} > \text{Cl} > \text{I}$.

Similarly, in trialkoxyphenyl isocyanide derivatives L^{C} , the high number of alkoxy chains makes very improbable that they (and their aryl rings) are reasonably confined close to the plane. Consequently, the breadth of the molecule will be determined essentially by the packing of the nonplanar trialkoxyphenyl groups and should be the same for all the halogens, as obtained by X-ray data. In this case the molecule with the best multicharge interactions should produce, as observed, the higher transition temperatures.

In summary, the binuclear copper(I) isocyanide complexes prepared exhibit mesogenic behavior and provide the first

(45) Gray, G. W. In *Liquid Crystals & Plastic Crystals*; Gray, G. W., Winsor, P. A., Eds.; John Wiley: New York, 1974; Vol. 1, Chapter 4.

Binuclear Mesogenic Copper(I) Isocyanide Complexes

examples of liquid crystals with a core formed by two tetrahedra sharing an edge. The shape of the molecule, which is mainly dominated by the organic ligand, permits a control of the mesogenic behavior, while the length of the chains and the use of different halogens provide a fine-tuning of the thermal properties.

Acknowledgment. We thank the Dirección General de Investigación (Project MAT2002-00562) and the Junta de Castilla y León (Projects VA15/00B and VA050/02) for financial support.

IC025703R